An *E*-Field Integral Equation Solution for the Radiation from Reflector Antennas with Struts

DAVID C. JENN, MEMBER, IEEE, AND WILLARD V. T. RUSCH, FELLOW, IEEE

Abstract—**The *E*-field integral equation is applied to rotationally symmetric reflector antennas with struts. Current is allowed to flow on all the reflector surfaces and continuity is enforced at the conductor junctions. Radiation patterns are presented for a small paraboloid antenna, and the effects of the struts are clearly identified. These include the strut cone radiation, pattern asymmetries introduced by the struts, and gain loss and sidelobe level changes.**

I. Introduction

THE BLOCKING OF a main reflector surface by subreflectors, feed horns, and struts causes significant changes in its radiation pattern. To date many approximate analytical techniques have been applied to this problem [1]–[8]. Equivalent currents or projected aperture methods are commonly used to predict the pattern changes due to subreflectors and struts. The geometrical theory of diffraction (GTD) is often used to estimate the wide angle sidelobe level. All these methods are high-frequency approximations that are only valid in certain angular regions. Furthermore, the interactions between the surfaces are neglected, as is current flow between two conductors at an attachment point. Hence, the present reflector theory is a conglomeration of approximations, each applied in a specific regime of frequencies and spatial sectors.

The method described here is based on the *E*-field integral equation (EFIE), which is exact in its formulation. It can be applied to any conducting body, multiple bodies in proximity to each other, or multiple bodies connected by wires. Thus, the total reflector problem can be solved by a single method that is valid at all frequencies and angles. The present formulation constitutes the first exact solution for the radiation from reflector antennas with struts. Although the method can be applied to any arbitrary geometry, several limitations will be imposed to reduce the complexity of the solution. It will be assumed that the strut cross section is small enough so that the thin wire approximation is satisfied. Also, the reflector surfaces must be axially symmetric, and the feed aperture blockage will be neglected. The latter is justified on the grounds that the investigation of strut scattering is the primary topic of this study, rather than the aperture blocking effects.

Manuscript received December 4, 1987; revised June 22, 1988.

D. C. Jenn is with the Ground Systems Group, Hughes Aircraft Company, P.O. Box 3310, Fullerton, CA 92634-3310.

W. V. T. Rusch is with the Department of Electrical Engineering, University of Southern California, Los Angeles, CA 90089.

IEEE Log Number 8927257.

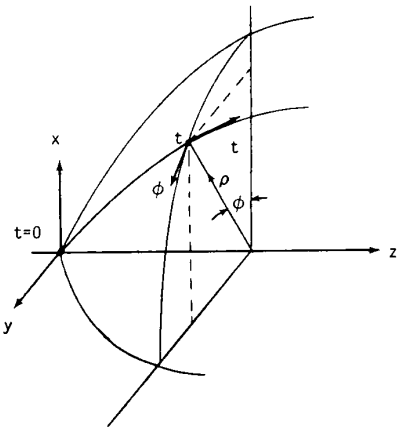

Fig. 1. BOR coordinate system.

II. Method of Analysis

Since the antenna configurations considered here will be limited to those with rotationally symmetric reflector surfaces, the problem reduces to one of scattering from a body of revolution (BOR) with wires conductively attached. Integral equation solutions to this problem have been presented by several authors [9]–[11]. The EFIE is derived from Maxwell's equations and the boundary conditions [12], and applies to any arbitrarily shaped infinitely thin perfectly conducting surface. The method of moments (MM) is used to reduce this integrodifferential equation to a set of simultaneous linear equations that can be solved to obtain the current on the surfaces. Once the currents are known the scattered field, and hence the total radiated field, can be computed.

The MM solution for the antenna surface currents is the same as that used by Mautz and Harrington [13], [14]. The reflector surfaces are divided into annular rings concentric with the axis of symmetry. A curvilinear coordinate system (t, ϕ) is established on the surface as shown in Fig. 1. The current is expanded in terms of a product of overlapping triangles or pulses and Fourier modes as follows:

$$\mathbf{J}_i^t = \mathbf{t}\, T_i(t)\, \frac{e^{-jn\phi}}{\rho}, \qquad i = 1, 2, \cdots, \text{number of triangles,} \tag{1}$$

$$\mathbf{J}_i^\phi = \boldsymbol{\phi}\, P_i(t)\, \frac{e^{-jn\phi}}{\rho_i}, \qquad i = 1, 2, \cdots, \text{number of pulses.} \tag{2}$$

$T_i(t)$ and $P_i(t)$ are the commonly used triangle and pulse

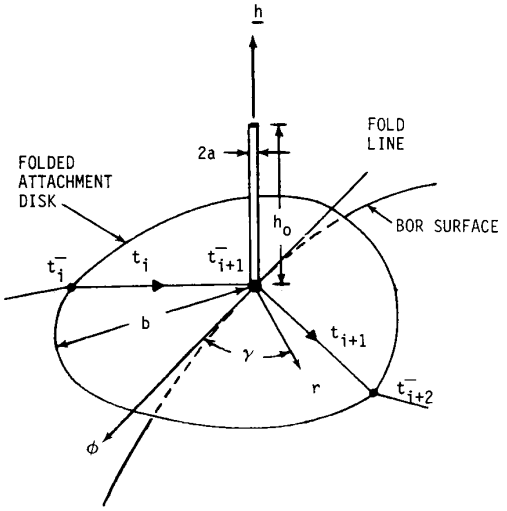

Fig. 2. Details of the junction region.

functions [14], and $\mathbf{t}$ and $\boldsymbol{\phi}$ are unit vectors. The time harmonic factor $e^{j\omega t}$ has been suppressed. In (1) and (2) $n = 0, \pm 1, \pm 2, \cdots, \pm\infty$.

Similar to the BOR, the strut is divided into segments and triangular expansion functions are defined

$$\mathbf{J}_j^w = \mathbf{h}_j T_j(h)/(2\pi a). \tag{3}$$

The index j runs over all strut basis functions, h is an arclength variable along the axis of the strut, and $\mathbf{h}_j$ a unit vector directed along the axis of the jth segment. It is assumed that the strut radius a is much smaller than the physical length and the wavelength, and therefore only an axial current will be present. This is often referred to as the thin wire approximation [15], [16].

The method of handling the junction is similar to the one used by Shaffer and Mitschang [9]. The approximation for the junction region consists of an attachment segment on the strut (the segment closest to the junction) and an attachment disk, which are shown in Fig. 2. The coordinates of the attachment point in the BOR coordinate system are (ρ_a, ϕ_a, z_a), and it is folded in the junction plane $\phi = \phi_a$. It approximates the BOR surface in the junction region. A polar coordinate system (r, τ) is defined on the disk, where γ is measured from the $z = z_a$ plane and $\mathbf{r}$ lies on the disk and points outward from the attachment point. Current is allowed to flow radially outward from the junction and is forced to decay to zero at the edge of the disk. The basis function is constructed to have the proper $1/r$ radial dependence

$$\mathbf{J}_d = -\mathbf{r}(b-r)/[2\pi r(b-a)] \tag{4}$$

where b is the disk radius. The expansion function for the attachment segment (half a triangle) prevents the strut current from going to zero at the attachment point

$$\mathbf{J}_a = \mathbf{a} T_a(h)/(2\pi a). \tag{5}$$

The unit vector $\mathbf{a}$ is directed outward along the attachment segment. Equations (4) and (5) have been scaled so that Kirchhoff's current law is satisfied at the junction ($r = a$).

Now, following the method of moments, the total current on the body is expressed as a superposition of all of the basis functions

$$\mathbf{J} = \sum_n \sum_i (I_{ni}^t \mathbf{J}_{ni}^t + I_{ni}^\phi \mathbf{J}_{ni}^\phi) + \sum_j I_j^w \mathbf{J}_j^w + \sum_l I_l^d \mathbf{J}_l^d \tag{6}$$

where n, i, j and l take on all possible values. Weighting (testing) functions are chosen according to Galerkin's method. The testing operation is used to reduce the EFIE to a set of linear equations that can be written in matrix form as

$$\mathbf{ZI} = \mathbf{V}. \tag{7}$$

The current vector $\mathbf{I}$ contains the unknown coefficients in the expansion (6). Equation (7) is actually an infinite set of equations, but can be reduced to a finite set by choosing a maximum value for n based on some convergence criteria.

Since any given current must be tested with all the weighting functions, nine distinct types of impedance elements result

$$\mathbf{Z}^{ss}, \mathbf{Z}^{ww}, \mathbf{Z}^{jj} \quad \text{(self-terms)}$$

$$\mathbf{Z}^{sw}, \mathbf{Z}^{ws}, \mathbf{Z}^{sj}, \mathbf{z}^{js}, \mathbf{Z}^{wj}, \mathbf{Z}^{jw} \quad \text{(interaction terms)}.$$

The superscripts s, w, and j refer to surface, wire (i.e., strut) and junction, respectively. The matrix equation (7) can be rewritten as

$$\begin{bmatrix} \mathbf{Z}^{ss} & \mathbf{Z}^{sw} & \mathbf{Z}^{sj} \\ \mathbf{Z}^{ws} & \mathbf{Z}^{ww} & \mathbf{Z}^{wj} \\ \mathbf{Z}^{js} & \mathbf{Z}^{jw} & \mathbf{Z}^{jj} \end{bmatrix} \begin{bmatrix} \mathbf{I}^s \\ \mathbf{I}^w \\ \mathbf{I}^j \end{bmatrix} = \begin{bmatrix} \mathbf{V}^s \\ \mathbf{V}^w \\ \mathbf{V}^j \end{bmatrix}. \tag{8}$$

The impedance blocks relating to the surfaces actually consist of several submatrices, one for each mode number n. As pointed out in [9] the impedance matrix takes on the following block structure:

$$\mathbf{Z} = \left[\begin{array}{ccccc:cc} \mathbf{Z}_M^{ss} & & & & & \mathbf{Z}_M^{sw} & \mathbf{Z}_M^{sj} \\ & \ddots & & & & \vdots & \vdots \\ & & \mathbf{Z}_0^{ss} & & & \mathbf{Z}_0^{sw} & \mathbf{Z}_0^{sj} \\ & & & \ddots & & \vdots & \vdots \\ & & & & \mathbf{Z}_{-M}^{ss} & \mathbf{Z}_{-M}^{sw} & \mathbf{Z}_{-M}^{sj} \\ \hdashline \mathbf{Z}_M^{ws} & \cdots & \mathbf{Z}_0^{ws} & \cdots & \mathbf{Z}_{-M}^{ws} & \mathbf{Z}^{ww} & \mathbf{Z}^{wj} \\ \mathbf{Z}_M^{js} & \cdots & \mathbf{Z}_0^{js} & \cdots & \mathbf{Z}_{-M}^{js} & \mathbf{Z}^{jw} & \mathbf{Z}^{jj} \end{array}\right] \tag{9}$$

where M is the magnitude of the highest mode number (i.e., $n = 0, \pm 1, \cdots, \pm M$). The detailed expressions for the impedance elements $\mathbf{Z}$ are given in [9] for the BORs, wires, junctions, and their interactions.

The elements of the excitation vector $\mathbf{V}$ are defined by

$$V_i^p = \frac{1}{\eta} \iint \mathbf{W}_i^p \cdot \mathbf{E}_f \, ds \tag{10}$$

where $p = s$, w or j and $\mathbf{E}_f$ is the primary feed field, which is located at the origin of the BOR coordinate system. For reasons mentioned earlier, blocking by the feed aperture will be neglected. In general, the far field of an arbitrary feed

radiating in the $-z$ direction can be represented by

$$\mathbf{E}_f = \begin{cases} \{\theta \cos\phi F_E(\theta) + \phi \sin\phi F_H(\theta)\} \dfrac{e^{-jkR}}{R}, & \theta > 90° \\ 0, & \theta \le 90° \end{cases} \tag{11}$$

where θ and ϕ are unit vectors and R is the distance from the feed to a point on the antenna surface. The functions F_E and F_H define the feed taper in the E- ($\phi = 0°$) and H-planes ($\phi = 90°$), respectively. Since the source is on the axis of symmetry only the $n = \pm 1$ modes of the BOR excitation vector are nonzero, but because of the presence of the struts, the azimuthal modes are not decoupled as they would be for a pure BOR. Thus, the interaction of the struts with the reflector surfaces will generate higher order BOR currents. The derivation of the excitation vector and the far-field relationship to the current is discussed in detail in [17].

The excitation of higher order modes substantially increases the dimension of the impedance matrix and restricts the size of the antenna that can be analyzed. Partitioning is used to reduce the size of the largest matrix that must be inverted. The particular method use here is based on Woodbury's identity [18], [19]

$$(\mathbf{A}+\mathbf{UPW})^{-1} = \mathbf{A}^{-1} - \mathbf{A}^{-1}\mathbf{U}(\mathbf{P}+\mathbf{WA}^{-1}\mathbf{U})^{-1}\mathbf{WA}^{-1}. \tag{12}$$

All the multiplications in (12) are outer products, and the matrices must be conformable and nonsingular. For the present application let $\mathbf{P} = \mathbf{I}$ (the identity matrix) so $\mathbf{Z} = (\mathbf{A} + \mathbf{UIW})$. The impedance matrix (9) is in the form

$$\left[\begin{array}{cccc|c} \mathbf{A}_1 & & & & \mathbf{B}_1 \\ & \mathbf{A}_2 & & & \mathbf{B}_2 \\ & & \ddots & & \vdots \\ & & & \mathbf{A}_s & \mathbf{B}_s \\ \hline \mathbf{C}_1 & \mathbf{C}_2 & \cdots & \mathbf{C}_s & \mathbf{D} \end{array}\right] \tag{13}$$

where

$$\mathbf{B}_n = [\mathbf{Z}_n^{sw}\ \mathbf{Z}_n^{sj}] \tag{14}$$

$$\mathbf{C}_n = \begin{bmatrix} \mathbf{Z}_n^{ws} \\ \mathbf{Z}_n^{js} \end{bmatrix} \tag{15}$$

$$\mathbf{A}_n = [\mathbf{Z}_n^{ss}] \tag{16}$$

and the subscript $s = 2M + 1$. Letting

$$\mathbf{U} = \begin{bmatrix} \mathbf{B}_1 & \mathbf{0} \\ \mathbf{B}_2 & \mathbf{0} \\ \vdots & \vdots \\ \mathbf{B}_s & \mathbf{0} \\ \mathbf{0} & \mathbf{I} \end{bmatrix} \tag{17}$$

$$\mathbf{W} = \begin{bmatrix} \mathbf{0} & \mathbf{0} & \cdots & \mathbf{0} & \mathbf{I} \\ \mathbf{C}_1 & \mathbf{C}_2 & \cdots & \mathbf{C}_s & \mathbf{0} \end{bmatrix} \tag{18}$$

and

$$\mathbf{A} = \begin{bmatrix} \mathbf{A}_1 & & & & \\ & \mathbf{A}_2 & & & \\ & & \ddots & & \\ & & & \mathbf{A}_s & \\ & & & & \mathbf{D} \end{bmatrix} \tag{19}$$

in (12) yields

$$\mathbf{Z}^{-1} = \left[\begin{array}{c|c} \mathbf{A}_j^{-1}\delta_{ij} - \mathbf{A}_i^{-1}\mathbf{B}_i\mathbf{X}_2\mathbf{C}_j\mathbf{A}_j^{-1} & -\mathbf{A}_i^{-1}\mathbf{B}_i\mathbf{X}_1\mathbf{D}^{-1} \\ \hline -\mathbf{D}^{-1}\mathbf{X}_4\mathbf{C}_j\mathbf{A}_j^{-1} & \mathbf{D}^{-1} - \mathbf{D}^{-1}\mathbf{X}_3\mathbf{D}^{-1} \end{array}\right] \tag{20}$$

where i and j represent the index of the i, jth submatrix and take on values from 1 to s. The partitions correspond to those in (9) and (13) and δ_{ij} is the Kronecker delta. The $\mathbf{X}_k$ are determined from

$$\mathbf{X} = (\mathbf{I} + \mathbf{WA}^{-1}\mathbf{U})^{-1} \tag{21}$$

$$\mathbf{X} = \begin{bmatrix} \mathbf{X}_1 & \mathbf{X}_2 \\ \mathbf{X}_3 & \mathbf{X}_4 \end{bmatrix} \tag{22}$$

$$\mathbf{X} = \begin{bmatrix} \mathbf{I} & \mathbf{D}^{-1} \\ \sum_{k=1}^{s} \mathbf{C}_k\mathbf{A}_k^{-1}\mathbf{B}_k & \mathbf{I} \end{bmatrix}^{-1}. \tag{23}$$

Because of the symmetry between the impedance elements

$$\mathbf{C}_n = \tilde{\mathbf{B}}_{s+1-n} \tag{24}$$

where the tilde denotes the matrix transpose.

The number of rows and columns in the original impedance matrix (9) is

$$N\text{ROW} = (2M+1)N + NWJ \tag{25}$$

where

NW	number of triangles on the struts
NJ	number of junctions
NWJ	$NW + NJ$
N	total number of BOR basis functions (triangles and pulses).

Thus the largest matrix that must be inverted when using Woodbury's identity is the largest of $N \times N$ or $(2NWJ) \times (2NWJ)$. This is much more manageable than that required to solve (9), because NROW could easily be 1000 for even a ten wavelength paraboloid.

III. Radiation Patterns

The radiation patterns were calculated for the 10 λ (λ is wavelength) prime focus paraboloid shown in Fig. 3. The axes of the struts are at an angle α_s with respect to the z axis. There are three struts spaced 120° apart. The reflector edge angle is 64° and the edge taper is approximately 7 dB. Fig. 4 compares the field scattered from the reflector only to that scattered from the reflector with struts. Three different strut radii are shown for $\alpha_s = 50.2°$. The total E-plane field is plotted in Fig. 5;

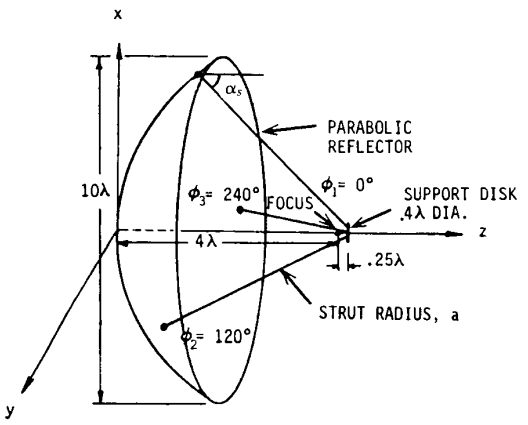

Fig. 3. Paraboloidal reflector with three equiangular struts.

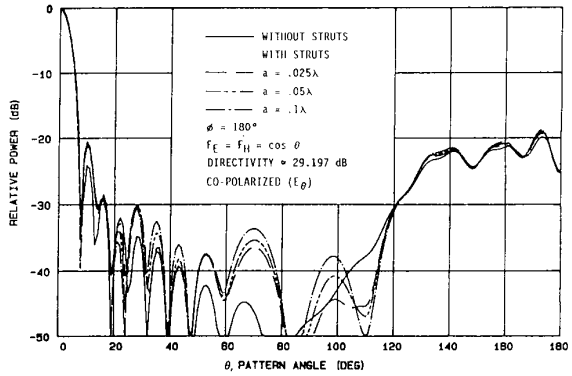

Fig. 4. Field scattered from a 10 λ paraboloidal reflector with and without struts.

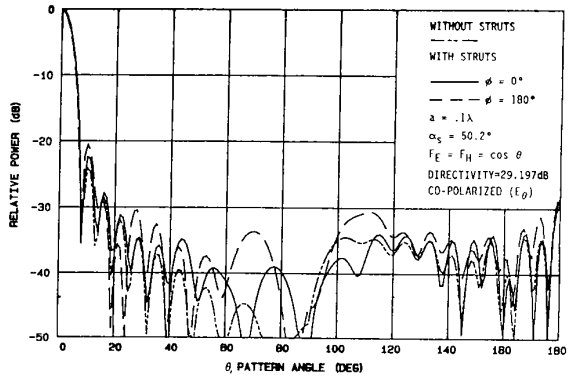

Fig. 5. E-plane field of a 10 λ paraboloid with and without struts.

that is, the field scattered by the reflector surfaces and radiated by the feed. A comparison of Figs. 4 and 5 shows that the feed field cancels much of the scattered field in the rear hemisphere. The asymmetry introduced by the struts is evident in comparing the $\phi = 0°$ and 180° patterns of Fig. 5. Because of the strut placement the H-plane pattern is identical for the $\phi = 90°$ and 270° planes, as shown in Fig. 6. Normally for a paraboloidal reflector without struts the cross polarization in the principal planes is zero. When struts are added, a nonzero cross-polarized field can result, as shown in Fig. 7 for the H-plane. The cross polarization in the E-plane, however, remains below −50 dB.

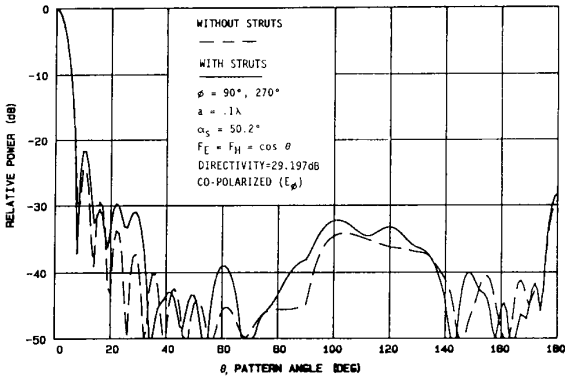

Fig. 6. H-plane field of a 10 λ paraboloid with and without struts.

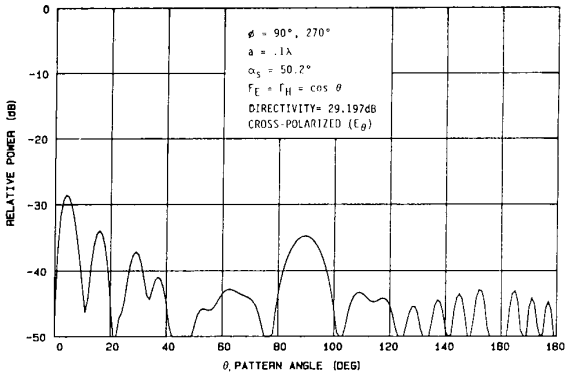

Fig. 7. H-plane cross-polarized field of a 10 λ paraboloid with struts.

TABLE I
CALCULATED GAIN LOSS AS A FUNCTION OF STRUT RADIUS

Method	Strut Radius	Gain Loss (dB)
EFIE	Without Struts	Reference
EFIE	a = 0.025 λ	0.096
EFIE	a = 0.050 λ	0.278
EFIE	a = 0.100 λ	0.392
IFR	a = 0.100 λ	0.385

One method commonly used to establish the gain loss from strut blockage is based on the induced field ratio (IFR) hypothesis [20]. The field scattered from the struts is assumed to be that excited by the plane-wave component of the focal-region field. The formulas relating gain loss and sidelobe level to the strut radius are given in [21]. For a cos θ feed pattern and a strut radius of 0.1 λ the resulting loss is 0.385 dB, which is close to the MM value of 0.392 dB. Table I lists the gain loss as a function of strut radius as obtained from the EFIE and IFR calculations.

The IFR approach also provides a means of estimating of the co- and cross-polarized sidelobe levels [22]. For $\phi = 0°$ the IFR predicts a first-sidelobe level of −22 dB, which is close to the MM result shown in Fig. 5. The IFR estimate for the peak cross-polarized level in the this plane is −35 dB, but

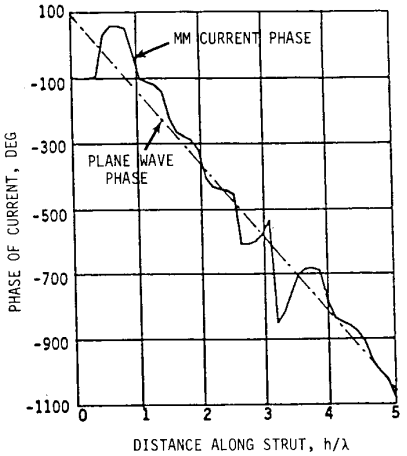

Fig. 8. Phase of the current induced on the strut.

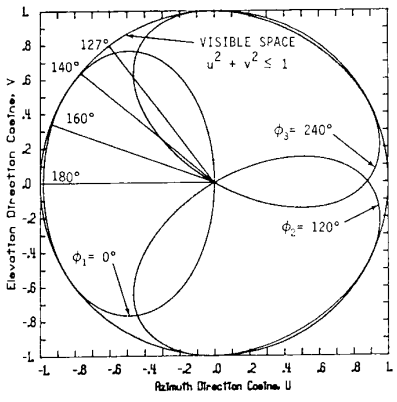

Fig. 9. Strut cone contours for three equi-angular struts at an angle of 50.2° with respect to the BOR z axis.

the MM level of -28 dB is significantly higher. The discrepancy is probably due to violation of the basic IFR assumption; that is, the plane wave component of the focal region field dominates. Actually reflections from the ends of the struts and feed illumination will corrupt the plane wave structure along the strut. This is illustrated by examining the phase of the strut current. If the plane wave field dominates then the phase should be linear across its length (L) with a total change of $kL \cos \alpha_s$. Fig. 8 shows the phase of the current along the $\phi = 0°$ strut for $a = 0.025\ \lambda$, $L = 5.075\ \lambda$ and $\alpha_s = 50.2°$. In spite of the apparently erratic phase due to the other components of the focal region field, the least squares slope is 226 degrees per wavelength along the strut, which is close to the plane wave phase of 230 degrees per wavelength.

The effect of the struts on the radiation pattern is usually most notable at wide angles. According to the IFR hypothesis, the effect at wide angles can be estimated assuming the strut excitation is dominated by the plane wave component of the field in the focal space of the reflector. When these induced currents are integrated, the radiation is locally maximum on cones which lie along the axis of each strut. The calculated position, width, and intensity of these so-called "strut cones" has been in good agreement with measured data [20]. The strut cone contours are plotted in Fig. 9 for the paraboloidal

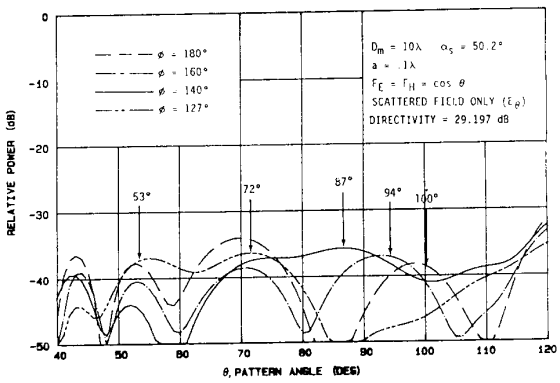

Fig. 10. Comparison of predicted strut cone locations with calculated pattern data for several planes ($\alpha_s = 50.2°$).

TABLE II
COMPUTER TIME TO SOLVE FOR THE CURRENTS ON A 10 λ PARABOLOID WITH STRUTS

Solution Method	Modes (M)	Computer Time (min) IBM 3083	CRAY X-MP/48	Largest Matrix Inversion
Direct	1	—	2.7	694 × 694
	2	*	*	1064 × 1064
	3	*	*	1434 × 1434
Woodbury's Identity	1	53	17	278 × 278
	2	115	33	278 × 278
	3	198	—	278 × 278

— Calculation not performed
* Calculation not possible because of insufficient memory

reflector of Fig. 3 with $\alpha_s = 50.2°$. The curves are the projections of the radiation maxima onto the x-y plane, and therefore some of the points actually lie behind the reflector ($\theta > 90°$). The x and y direction cosines are $u = \sin\theta \cos\phi$ and $v = \sin\theta \sin\phi$, respectively.

Fig. 10 shows the radiation patterns in the ϕ planes that correspond to those indicated in Fig. 9. The expected strut cone locations are marked by arrows. These maxima generally agree with those shown in Fig. 9. The fact that they are not well defined is not surprising in view of the strut phase behavior in Fig. 8. Even if the phase errors were not present, the intensity of the cones is not significantly greater than the scattered field from the reflector surface, because the struts are thin. (The lobe intensity increases with the radius of the strut, as can be seen by comparing the lobe at 100° in the scattered field patterns of Fig. 4.) In directions where the contribution from the reflector is smaller the strut lobes do dominate (for instance, the strut cone at $\theta = 90°$ in the cross-polarization pattern of Fig. 7). Similar calculations with other strut angles were also in agreement with the IFR locations, and as predicted by the IFR formulas the strut cones shift toward the main beam for smaller α_s.

IV. Computer Considerations

The antenna calculations were done on IBM 3083 and CRAY X-MP/48 computers. The run times for several cases are shown in Table II. Without the use of Woodbury's identity

TABLE III
MAIN BEAM VALUE VERSUS NUMBER OF AZIMUTHAL BOR MODES FOR THE REFLECTOR OF FIG. 3 WITH $a = 0.025\ \lambda$ AND $F_E = F_H = \cos\theta$

Configuration	M*	Gain (db)
Reflector only	1	29.197
Reflector and disk	1	29.190
Reflector with struts	1	29.138
Reflector with struts	2	29.093
Reflector with struts	3	29.093

* Modes: $n = 0, \pm 1, \cdots, \pm M$

to partition the impedance matrix, the calculation of even 10 λ diameter reflectors would not be possible on the particular computer systems used here. No special effort was made to optimize the software to take advantage of the CRAY architecture. However, significant reductions in time probably would not occur because most of it is due to read/write operations to disk files.

The sensitivity and convergence of the solution was tested as a function of several parameters: number of azimuthal BOR modes, attachment disk size, and MM subsection size. Mode convergence was tested using three, five, and seven azimuthal BOR modes. From [9] the magnitude of the highest required mode number should be

$$M \geq 2\pi/\phi_m = 3 \tag{26}$$

since $\phi_m = 120°$ is the angular separation between struts. The convergence of the main beam value is given in Table III. The results for five and seven modes were within 0.2 dB of each other down to the −40 dB level.

The results will depend to some extent on the attachment disk radius. Since the junction area is small compared to the total reflector surface, it is expected that the choice of attachment disk radius is not critical in calculating the main beam maximum or even the first several sidelobes. In an effort to estimate the sensitivity of the field to the junction parameters, calculations were done for several disk sizes. Although the radius differs slightly at each attachment point, the average value used in all the calculations shown was 0.15 λ. Additional calculations were done for an average radius of 0.3 λ and for no current flow at the junction ($b = 0$). Either way there was no significant change down to the −30 dB level, and only a 1 to 2 dB change below the −30 dB level. Interestingly enough, if reducing the attachment disk radius lowered a particular wide angle sidelobe, then increasing the disk radius would raise it and vice versa.

The effect of the surface and strut segment size was also investigated. Because of computer memory limitations, the segments could not be reduced indefinitely. The smallest segment size that could be handled was about 0.08 λ (for both the reflector surfaces and the struts). Increasing these to 0.12 λ caused small changes ($\simeq 1$ dB) in the −35 to −50 dB range, and also a slight shift in some of the wide angle sidelobe positions.

V. SUMMARY

The EFIE has been applied to rotationally symmetric antennas and radiation patterns were calculated for a 10 λ paraboloid with struts. The IFR hypothesis was used to predict the strut cone radiation maxima. The co-polarized sidelobe positions that were calculated for this paraboloid were in agreement with the expected locations. Evidently, in this case, the plane wave component is the major contributor to the focal-region field even though a reflector this size is considered electrically small.

In principle this solution is applicable to reflectors of any size and the extension to dual surfaces is straightforward. The thin wire limitation on the struts can be removed by allowing higher order circumferential currents. Thus computer size is the major limiting factor in extending this solution to electrically large antennas.

ACKNOWLEDGMENT

The authors would like to thank the San Diego Supercomputer Center at the University of California, San Diego, for the grant of computer time. Also Professor R. F. Harrington, Syracuse University, for providing the BOR computer program on which the present work is based, and Professor G. H. Golub, Stanford University, for his suggestions on matrix partitioning.

REFERENCES

[1] G. L. James and V. Kerdemelidis, "Reflector antenna radiation pattern analysis by equivalent edge currents," *IEEE Trans. Antennas Propagat.*, vol. AP-21, no. 1, p. 19, Jan. 1973.
[2] S. H. Lee *et al.*, "A GTD analysis of the circular reflector antenna including feed and strut clutter," The Ohio State Univ. ElectroSci. Lab., Dept. Elec. Eng., Columbus, Rep. 4381-1, May 25, 1977.
[3] ——, "Feed strut analysis for wide angle sidelobes," in *1984 IEEE Antennas Propagat. Soc. Int. Symp. Dig.*, vol. AP 2(a)-2, June 1984, p. 63.
[4] C. L. Gray, "Estimation of the effect of feed support member blocking on antenna gain and sidelobe level," *Microwave J.*, vol. 7, no. 3, p. 88, Mar. 1964.
[5] J. Ruze, "Feed support blockage loss in parabolic antennas," *Microwave J.*, vol. 11, no. 12, p. 76, Dec. 1968.
[6] W. V. T. Rusch *et al.*, "Forward scattering from square cylinders in the resonance region with application to aperture blockage," *IEEE Trans. Antennas Propagat.*, vol. AP-24, no. 2, p. 182, Mar. 1976.
[7] J. H. Wested, "Shadow and diffraction effect of spars in a Cassegrain system," Microwave Lab., Danish Academy of Tech. Studies, Rep. P2118, Mar. 1966.
[8] J. Dijk, M. Jeuken, and E. J. Maanders, "Blocking and diffraction in Cassegrain antenna systems," Technological Univ.—Eindhoven (Netherlands), *De Ingenieur*, no. 27, p. 79, July 1968.
[9] J. R. Shaeffer and L. N. Medgyesi-Mitschang, "Radiation from wire antennas attached to bodies of revolution: The junction problem," *IEEE Trans. Antennas Propagat.*, vol. AP-29, no. 3, p. 479, May 1981.
[10] N. C. Albertsen, J. E. Hansen, and N. E. Jensen, "Computation of radiation from wire antennas on conducting bodies," *IEEE Trans. Antennas Propagat.*, vol. AP-22, no. 2, p. 200, Mar. 1974.
[11] E. H. Newman and D. M. Pozar, "Electromagnetic modeling of composite wire and surface geometries," *IEEE Trans. Antennas Propagat.*, vol. AP-26, no. 6, Nov. 1978.
[12] J. R. Mautz and R. F. Harrington, "Radiation and scattering from bodies of revolution," *Appl. Sci. Res.*, vol. 20, p. 405, June 1969.
[13] ——, "*H*-field, *E*-field, and combined field solutions for bodies of revolution," Syracuse Univ., Syracuse, NY, Tech. Rep. TR-77-2, Feb. 1977.
[14] ——, "An improved *E*-field solution for a conducting body of revolution," Syracuse Univ., Syracuse, NY, Tech. Rep. TR-80-1.
[15] J. H. Richmond, "Digital computer solutions of the rigorous equations for scattering problems," *Proc. IEEE*, vol. 54, no. 8, p. 796, Aug. 1965.
[16] C. M. Butler and D. R. Wilton, "Analysis of various numerical techniques applied to thin-wire scatterers," *IEEE Trans. Antennas Propagat.*, vol. AP-23, no. 4, p. 534, July 1975.
[17] D. C. Jenn, "The application of integral equation theory to reflector

antenna analysis," Ph.D. dissertation, Univ. Southern California, Dec. 1987.
[18] A. D. Whalen, *Detection of Signals in Noise.* New York: Academic, 1971, p. 364.
[19] G. H. Golub and C. F. Van Loan, *Matrix Computations.* Baltimore, MD: Johns Hopkins Univ. Press, 1983.
[20] W. V. T. Rusch, O. Sorensen, and J. W. M. Baars, "Radiation cones from feed-support struts of symmetric paraboloidal antennas," *IEEE Trans. Antennas Propagat.*, vol. AP-30, no. 4, p. 786, July 1982.
[21] P. S. Kildal, E. Olsen, and J. A. Aas, "Losses, sidelobes and cross polarization caused by feed-support struts in reflector antennas: Design curves," *IEEE Trans. Antennas Propagat.*, vol. 36, no. 2, p. 182, Feb. 1988.
[22] W. V. T. Rusch and O. Sorensen, "Aperture blocking of a focused paraboloid," Lab. Electromagn. Theory, Tech. Univ. Denmark, Lyngby, Rep. R 126, July 31, 1974.

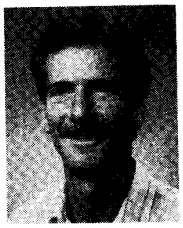

David C. Jenn (S'75–A'79–M'82) was born in Sioux City, IA, on August 24, 1952. He received the B.S. degree from the University of Wisconsin-Milwaukee in 1975, the M.S. degree from The Ohio State University, Columbus, in 1976, and the Ph.D. degree from the University of Southern California, Los Angeles, in 1987.

From 1976 to 1978 he was with the McDonnell-Douglas Astronautics Co., St. Louis, MO, where he was involved primarily in the design of small arrays and radomes for airborne radar altimeters. Since 1978 he has been with Hughes Aircraft Co., Fullerton, CA, where he has contributed to the design and analysis of phased array antennas used in various radar and communication systems. Most recently his work has concentrated on method of moment solutions to scattering by complex bodies.

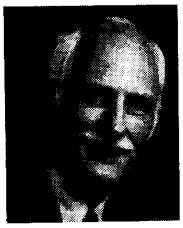

Willard V. T. Rusch (S'56–M'60–SM'73–F'76) received the B.S.E. degree from Princeton University, Princeton, NJ, in 1954, and the M.S. and Ph.D. degrees from the California Institute of Technology, Pasadena, in 1955 and 1959, respectively, all in electrical engineering. During the period of his graduate study he was a National Science Foundation Fellow.

After graduation, he spent the 1959–1960 academic year as a Fulbright Scholar at the Institute of Technology, Aachen, Germany. In 1960 he joined the faculty of the University of Southern California, Los Angeles, where he is currently Professor of Electrical Engineering. In 1962 he was a Visiting Scientist at the Radio Astronomy Branch, Naval Research Laboratory, Washington, DC. In 1966–1967 he was a Member of the Technical Staff, Bell Telephone Laboratories, Holmdel, NJ. In 1973–1974 he was a Visiting Professor at the Electromagnetics Institute, Technical University at Denmark, Lyngby, Denmark. In 1980–1981 he was a Visiting Scientist at the Max Planck Institut fuer Radioastronomie, Bonn, Germany, during which time he received a U.S. Senior Scientist Prize from the Alexander von Humboldt Foundation. He has been a consultant for numerous aerospace companies and government organizations. He has authored or co-authored more than 120 articles, books, patents, and symposium papers on various aspects of applied electromagnetic theory, with particular emphasis on reflector antennas.

Dr. Rusch is a member of Phi Beta Kappa, Sigma Xi, Eta Kappa Nu, Tau Beta Pi, Blue Key, and the International Union of Radio Science Commission B. He has served as National Director for Eta Kappa Nu and as a member of the IEEE Antennas and Propagation Society Administrative Committee.